

## **Rosette-forming glioneuronal tumors share a distinct DNA methylation profile and mutations in *FGFR1*, with recurrent co-mutation of *PIK3CA* and *NF1***

Philipp Sievers<sup>1,2</sup>, Romain Appay<sup>3,4</sup>, Daniel Schrimpf<sup>1,2</sup>, Damian Stichel<sup>1,2</sup>, David E. Reuss<sup>1,2</sup>, Annika K. Wefers<sup>1,2</sup>, Annekathrin Reinhardt<sup>1,2</sup>, Roland Coras<sup>5</sup>, Viktoria Ruf<sup>6</sup>, Karin de Stricker<sup>7</sup>, Henning Boldt<sup>8</sup>, Bjarne Winther Kristensen<sup>8,9</sup>, Jeanette Krogh Petersen<sup>8</sup>, Benedicte P. Ulhøi<sup>10</sup>, Maria Gardberg<sup>11</sup>, Eleonora Aronica<sup>12,13</sup>, Martin Hasselblatt<sup>14</sup>, Wolfgang Brück<sup>15</sup>, Wolfgang Wick<sup>16,17</sup>, Christel Herold-Mende<sup>18</sup>, Daniel Hänggi<sup>19</sup>, Sebastian Brandner<sup>20,21</sup>, Felice Giangaspero<sup>22,23</sup>, David Capper<sup>24,25,26</sup>, Elisabeth Rushing<sup>27</sup>, Pieter Wesseling<sup>28,29</sup>, Stefan M. Pfister<sup>30,31,32</sup>, Dominique Figarella-Branger<sup>3,4</sup>, Andreas von Deimling<sup>1,2</sup>, Felix Sahm<sup>1,2,30\*</sup>, David T. W. Jones<sup>30,33\*</sup>

<sup>1</sup>Department of Neuropathology, Institute of Pathology, University Hospital Heidelberg, Heidelberg, Germany

<sup>2</sup>Clinical Cooperation Unit Neuropathology, German Consortium for Translational Cancer Research (DKTK), German Cancer Research Center (DKFZ), Heidelberg, Germany

<sup>3</sup>APHM, Hôpital de la Timone, Service d'Anatomie Pathologique et de Neuropathologie, Marseille, France

<sup>4</sup>Aix-Marseille Univ, CNRS, INP, Inst Neurophysiopathol, Marseille, France

<sup>5</sup>Department of Neuropathology, University of Erlangen-Nürnberg, Erlangen, Germany

<sup>6</sup>Department of Neuropathology, Ludwig-Maximilian University, Munich, Germany

<sup>7</sup>Department of Pathology, Rigshospitalet, Copenhagen, Denmark

<sup>8</sup>Department of Pathology, Odense University Hospital, Odense, Denmark

<sup>9</sup>Department of Clinical Research, University of Southern Denmark, Odense, Denmark

<sup>10</sup>Department of Pathology, Aarhus University Hospital, Aarhus, Denmark

<sup>11</sup>Department of Pathology University of Turku and Turku University Hospital, Turku, Finland

<sup>12</sup>Department of (Neuro)Pathology, Amsterdam UMC, University of Amsterdam, Amsterdam, The Netherlands

<sup>13</sup>Stichting Epilepsie Instellingen Nederland (SEIN), Zwolle, The Netherlands

<sup>14</sup>Institute of Neuropathology, University Hospital Münster, Münster, Germany

<sup>15</sup>Institute of Neuropathology, University Medical Center, Göttingen, Germany

<sup>16</sup>Clinical Cooperation Unit Neurooncology, German Consortium for Translational Cancer Research (DKTK), German Cancer Research Center (DKFZ), Heidelberg, Germany

<sup>17</sup>Department of Neurology and Neurooncology Program, National Center for Tumor Diseases, Heidelberg University Hospital, Heidelberg, Germany

<sup>18</sup>Division of Experimental Neurosurgery, Department of Neurosurgery, University Hospital Heidelberg, Heidelberg, Germany

<sup>19</sup>Department of Neurosurgery, University Medical Centre Mannheim, University of Heidelberg, Mannheim, Germany

<sup>20</sup>Division of Neuropathology, National Hospital for Neurology and Neurosurgery, University College London Hospitals NHS Foundation Trust, Queen Square, London, UK

<sup>21</sup>Department of Neurodegenerative Disease, UCL Queen Square Institute of Neurology, Queen Square, London, UK

<sup>22</sup>Department of Radiological Sciences, Oncology and Anatomical Pathology, Sapienza University Rome, Rome, Italy

<sup>23</sup>IRCCS Neuromed, Pozzilli, Italy

<sup>24</sup>Charité-Universitätsmedizin Berlin, Freie Universität Berlin, Humboldt-Universität zu Berlin, Berlin, Germany

<sup>25</sup>Institute of Neuropathology, Berlin Institute of Health, Berlin, Germany

<sup>26</sup>German Cancer Consortium (DKTK), Partner Site Berlin, Berlin, Germany

<sup>27</sup>Institute of Neuropathology, University Hospital Zurich, Zurich, Switzerland

<sup>28</sup>Department of Pathology, VU University Medical Center/Brain Tumor Center Amsterdam, Amsterdam, The Netherlands

<sup>29</sup>Department of Pathology, Princess Máxima Center for Pediatric Oncology and University Medical Center Utrecht, Utrecht, The Netherlands

<sup>30</sup>Hopp Children's Cancer Center at the NCT Heidelberg (KITZ), Heidelberg, Germany

<sup>31</sup>Division of Pediatric Neurooncology, German Cancer Consortium (DKTK), German Cancer Research Center (DKFZ), Heidelberg, Germany

<sup>32</sup>Department of Pediatric Oncology, Hematology, Immunology and Pulmonology, University Hospital Heidelberg, Heidelberg, Germany

<sup>33</sup>Pediatric Glioma Research Group, German Consortium for Translational Cancer Research (DKTK), German Cancer Research Center (DKFZ), Heidelberg, Germany

\* These authors share senior authorship

Corresponding authors:

Felix Sahm

[felix.sahm@med.uni-heidelberg.de](mailto:felix.sahm@med.uni-heidelberg.de)

David T. W. Jones

[david.jones@kitz-heidelberg.de](mailto:david.jones@kitz-heidelberg.de)

## Abstract

Rosette-forming glioneuronal tumor (RGNT) is a rare brain neoplasm that primarily affects young adults. Although alterations affecting the mitogen-activated protein kinase (MAPK) and phosphoinositide 3-kinase (PI3K) signaling pathway have been associated with this low-grade glioneuronal entity, comprehensive molecular investigations of RGNT in larger series have not been performed to date, and an integrated view of their genetic and epigenetic profiles is still lacking. Here we describe a genome-wide DNA methylation and targeted sequencing-based characterization of a molecularly distinct class of tumors ( $n = 30$ ), initially identified through genome-wide DNA methylation screening amongst a cohort of  $> 30,000$  tumors, of which most were diagnosed histologically as RGNT. *FGFR1* hotspot mutations were observed in all tumors analyzed, with co-occurrence of *PIK3CA* mutations in about two thirds of the cases (63%). Additional loss-of-function mutations in the tumor suppressor gene *NF1* were detected in a subset of cases (33%). Notably, in contrast to most other low-grade gliomas, these tumors often displayed co-occurrence of two or even all three of these mutations. Our data highlight that molecularly defined RGNTs are characterized by combined genetic alterations affecting both MAPK and PI3K signaling pathways. Thus, these two pathways appear to synergistically interact in the formation of RGNT, and offer potential therapeutic targets for this disease.

**Keywords:** Rosette-forming glioneuronal tumor, RGNT, Brain tumor, DNA methylation profile, Molecular classification, MAPK, PI3K, *FGFR1*, *PIK3CA*, *NF1*

## Introduction

Rosette-forming glioneuronal tumor (RGNT) is an uncommon central nervous system (CNS) neoplasm that primarily affects young adults [17]. It typically arises in the midline, usually occupying a substantial fraction of the fourth ventricle. In the World Health Organization (WHO) classification of brain tumors 2007, RGNT was therefore per definition associated with the fourth ventricle. However, more recent reports have shown that it can also affect other sites [1,2,17,25,29]. Thus, the extension "of the fourth ventricle" was abandoned in the current update of the classification [17].

Histologically, RGNT is characterized by a biphasic histologic architecture consisting of well-differentiated neurocytic cells forming rosettes or perivascular pseudorosettes and a glial component resembling pilocytic astrocytoma [9,14,19,23]. While large-scale genomic and epigenomic analyses over the past decade have immensely contributed to our understanding of molecular mechanisms underlying many primary brain tumors, current knowledge on the molecular background of RGNT is based mainly on individual case reports or small series. Targeted molecular analyses revealed absence of *KIAA1549-BRAF* fusions or activating *BRAF* mutations [6] which are a hallmark of pilocytic astrocytoma [10,11] and can also be found in other low-grade glial and glioneuronal tumors [30]. In contrast, activating mutations in *FGFR1* [7,16] and/or *PIK3CA* [3,5,16,28] have been described in a subset of RGNTs.

We here performed a combined (epi)genomic analysis of genome-wide DNA methylation profiling and targeted next-generation DNA sequencing data from 30 tumors in order to evaluate the underlying molecular background and to identify new diagnostic biomarkers as well as potentially targetable alterations.

## **Materials and methods**

### **Study population and sample collection**

Tumor samples and retrospectively determined clinical data from 30 patients were obtained from multiple international collaborating centers and collected at the Department of Neuropathology of the University Hospital Heidelberg (Heidelberg, Germany). Case selection was based on unsupervised hierarchical clustering of genome-wide DNA methylation data in a cohort of > 30,000 tumors that revealed a molecularly distinct group of tumors comprising 30 samples, of which the majority was diagnosed histologically as RGNT. Tissue was available for 24 cases thereof. Additionally, DNA methylation data of numerous well characterized reference samples representing CNS tumors of known histological and/or molecular subtype were used for comparative analyses [4]. Detailed descriptions of the reference methylation classes are outlined under <https://www.molecularneuropathology.org>. Tissue sample collection and processing, data collection, and use were performed in accordance with local ethics regulations and approvals. Clinical patient details are listed in Fig. 2 and Supplementary Table 1.

### **Histology and immunohistochemistry**

All samples with available tissue (n = 24/30) were histopathologically re-assessed according to the WHO 2016 classification of tumors of the central nervous system. Formalin-fixed, paraffin-embedded (FFPE) tissue samples were stained with hematoxylin and eosin (H&E) according to standard protocols. For all cases with sufficient material, immunohistochemistry was performed on a Ventana BenchMark ULTRA Immunostainer using either the OptiView DAB IHC Detection Kit or the ultraView Universal DAB Detection Kit (Ventana Medical Systems, Tucson, Arizona, USA). Antibodies were directed against: glial fibrillary acid protein (GFAP; Z0334, rabbit polyclonal, 1:1000 dilution, Dako Agilent, Santa Clara, CA, USA), Olig2 (clone EPR2673, rabbit monoclonal, 1:100 dilution, Abcam, Cambridge, UK), Synaptophysin (clone MRQ-40, rabbit monoclonal, 1:160 dilution, Cell Marque Corp., Rocklin, CA, USA), NeuN (clone A60, mouse monoclonal, 1:100 dilution, Millipore, Burlington, MA, USA), CD34 (clone QBEnd/10, mouse monoclonal, Ventana Medical Systems), Ki-67 (clone MIB-1, mouse monoclonal, 1:100 dilution, Dako Agilent).

### **DNA extraction**

Representative tumor tissue with highest available tumor cell content (~50-90%) was histologically identified and selected for nucleic acid extraction. Genomic DNA was extracted from fresh-frozen or formalin-fixed and paraffin-embedded (FFPE) tissue samples using the automated Maxwell system with the Maxwell 16 Tissue DNA Purification Kit or the Maxwell 16 FFPE Plus LEV DNA Purification Kit (Promega, Madison, WI, USA), according to the manufacturer's instructions.

### **DNA methylation array processing and copy number profiling**

The Infinium HumanMethylation450 (450k) BeadChip or Infinium MethylationEPIC (850k) BeadChip array (Illumina, San Diego, CA, USA) were used to obtain genome-wide DNA methylation profiles of tumor samples according to the manufacturer's instructions at the Genomics and Proteomics Core Facility of the German Cancer Research Center (DKFZ; Heidelberg, Germany). DNA methylation data were generated from both fresh-frozen and FFPE tissue samples. On-chip quality metrics of all samples were carefully controlled. Processing of DNA methylation data was performed with custom approaches as previously described [8,27]. Copy number profiles were generated using the 'conumee' package for the "R" environment (<http://bioconductor.org/packages/release/bioc/html/conumee.html>). All samples were checked for duplicates by pairwise correlation of the genotyping probes on the 450k/850k array.

### **Targeted next-generation DNA sequencing and mutational analysis**

Targeted exon capture and next-generation sequencing covering the coding regions of 130 genes of particular relevance in brain tumors was performed on a NextSeq 500 sequencer (Illumina) as previously described [24] for all tumor samples (n = 30). Fusion discovery was done based on panel sequencing data using deFuse [18] and arriba (<https://github.com/suhrig/arriba/>).

### **Statistical analysis**

DNA methylation array data were processed with the R/Bioconductor package minfi (version 1.20). For unsupervised hierarchical clustering of samples, the 20,000 most variably methylated probes by median absolute deviation across the dataset were selected. Samples were hierarchically clustered using Euclidean distance and Ward's linkage method. DNA methylation probes were reordered using Euclidian distance and complete linkage. For unsupervised 2D representation of pairwise sample correlations, dimensionality reduction by t-distributed stochastic neighbor embedding (t-SNE) was performed using the 20,000 most variable CpG sites according to standard deviation, a perplexity value of 10 and 3000 iterations. Survival data were analyzed by Kaplan-Meier analysis and compared by log-rank test using GraphPad Prism 8 (GraphPad Software, La Jolla, CA, USA). P values < 0.05 were considered significant.

## Results

### DNA methylation profiling highlights a distinct epigenetic signature of RGNT

Based on an unsupervised analysis of genome-wide DNA methylation data in a cohort of >30,000 tumors, we identified a molecularly distinct group of tumors forming a cluster separate from other established entities. The majority of these were diagnosed histologically as RGNT (Supplementary Table 1 and Fig. 2). A subsequent focused unsupervised hierarchical clustering and t-distributed stochastic neighbor embedding (t-SNE) analysis of DNA methylation patterns of these cases, alongside 106 well-characterized CNS neoplasms encompassing other low-grade glial/glioneuronal tumor entities and control tissue (white matter), consistently confirmed the distinct nature of this class (Fig. 1). This unique pattern supports the consideration of RGNT as a distinct molecular tumor type. Analysis of copy number variations (CNVs) calculated from the DNA methylation array data revealed a flat (=balanced) profile in most of the cases. Only single cases showed a small number of copy number alterations, with no obvious recurrent patterns.

### RGNTs are characterized by alterations affecting MAPK and PI3K signaling pathways

To investigate the mutational landscape in RGNT, we performed targeted next-generation sequencing on genomic DNA isolated from 30 tumors (Fig. 2 and Supplementary Table 1). In all analyzed tumors, a missense mutation within the kinase domain of *FGFR1* was identified – resulting in either a p.N546K (n = 22) or p.K656E (n = 8) substitution (details are listed in Supplementary Table 2). Both result in activating alterations within the kinase domain of *FGFR1* and were previously reported in other glioneuronal tumors [21]. Additionally, 19 of 30 (63%) of the *FGFR1*-mutant tumors harbored a concomitant mutation in *PIK3CA* which acts as an integral part of the PI3K pathway, including 14 with a p.H1047R, two with a p.E545K, and one each with a p.E542K, p.H1047L or p.G1049R substitution. The mutant allele frequency for the *FGFR1* and *PIK3CA* variants ranged from 23 to 58% / 23 to 48%, consistent with a heterozygous somatic mutation on the background of ~50-90% tumor purity (Supplementary Table 2).

Besides activating *FGFR1* and *PIK3CA* mutations, missense or damaging mutations in *NF1* were identified in 10 of the cases. Allele frequencies (13-55%) were consistent with being heterozygous somatic variants. No indication for a loss of heterozygosity was found by copy number analysis. Notably, seven of the tumors (23%) had a combined triple alteration of *FGFR1*, *PIK3CA* and *NF1* - indicating a cooperative role in tumorigenesis.

Two of the *FGFR1*-mutant tumors also harbored a *PTPN11* variant, typically altered in patients with Noonan syndrome. The *PTPN11* variants could not be verified as being in the germline because analysis was performed without matched normal tissue sample. In one of the cases, however, a Noonan syndrome was clinically known.

### Clinical characteristics and morphological features within the molecularly defined RGNT cohort

All cases were located infratentorially, preferentially in the posterior fossa occupying the 4<sup>th</sup> ventricle and the cerebellum. However, in line with other studies, the molecularly-defined

RGNTs described here also arose in mesencephalic or diencephalic regions [1,2,17,25,29]. Median age of the patients at the time of diagnosis was 32 years (range 10–69) and the sex distribution was balanced (male:female ratio 1.0). Basic clinical characteristics of the cases are summarized in Figure 2 and Supplementary Table 1. Outcome data were available for only ten patients. Analysis of overall survival (OS) of RGNT patients in comparison to reference glioma groups supports classification of the molecularly-rendered RGNT as WHO grade I, in line with the so far histologically-defined entity (Supplementary Fig. 1).

Histologically, all tumors were characterized by a moderate cellularity of neuroepithelial tumor cells. While a glial component consisting of spindle to stellate-shaped astrocytic cells with oval or elongated nuclei in a dense fibrillary background were seen in all tumors, populations of uniform neurocytic cells arranged in rosettes and perivascular pseudorosettes could be observed in only 20 of the 24 cases (Fig. 3). Neurocytic cells typically showed round nuclei with fine stippled chromatin dispersed in a mucoid or fibrillary matrix. In seven of the cases an oligodendroglioma-like cytology was seen focally. Some of the tumors demonstrated eosinophilic granular bodies (n = 9) or Rosenthal fibers (n = 8). Calcification were seen in a small number of tumors (n = 5). Hyalinized vessels and focal reactive vascular proliferation were observed in nine cases. Necrosis was uniformly absent. Mitotic activity was very low to absent. Immunoreactivity for synaptophysin was present in the neurocytic component (Fig. 3), whereas the glial component exhibited strong positivity for GFAP. The tumor cells were Olig2 positive and NeuN and CD34 negative. Proliferation index (Ki67) ranged from 1 to 3% in 22 of the cases, only two of the cases showed a slightly elevated proliferation index of up to 7 or 10%. Notably, all cases were histologically compatible with the diagnosis RGNT, although some cases would more likely have been favored as a typical differential diagnosis of RGNT.



## Discussion

Using genome-wide DNA methylation profiling, we have confirmed a highly distinct epigenetic signature of RGNT and shown that tumors within this group share recurrent alterations within the MAPK and PI3K/AKT/mTOR signaling pathways.

As alterations within the kinase domain of *FGFR1* were detected in all tumors analyzed, it seems that RGNTs are primarily driven by mutations leading to constitutive activation of FGFR signaling. Genetic alterations within the FGFR signaling pathway are also common in other low-grade glial and glioneuronal tumors, with missense mutations in *FGFR1*, internal tandem duplication of the kinase domain, and *FGFR1-TACC1* fusions being observed [10,20,21,26,30]. In contrast to those other tumor types, however, RGNT showed further recurrent mutations in the oncogene *PIK3CA*, which acts as an integral part of the PI3K pathway, and in the *NF1* tumor suppressor. Although these genes are each mutated in several other primary brain tumors, concomitant mutations (in such a high frequency as observed here) seem to be extremely uncommon, particularly in low-grade glioneuronal tumors. However, combined activation of MAPK and PI3K/AKT/mTOR signaling pathways has been previously reported in single cases of RGNT [7,16] and therefore appears to be highly characteristic of this molecular class. While *FGFR* alterations are also common in dysembryoplastic neuroepithelial tumor, another low-grade glioneuronal tumor with histological overlap to RGNT, no mutations of *PIK3CA* and only one concomitant *NF1* mutation were found in 32 analyzed cases.

Although there is no certain association with hereditary syndromes, RGNT has been described in patients with neurofibromatosis type 1 [13], as well as Noonan syndrome [12,16]. None of the *NF1* mutations in our cohort could be confirmed as being present in the germline, although only very few cases had germline material available. Two of the *FGFR1*-mutant tumors also displayed a *PTPN11* variant, typically altered in patients with Noonan syndrome. Although matched normal tissue samples were unfortunately not available for these cases, in one of them a Noonan syndrome had already been clinically diagnosed.

In comparison to the vast majority of other low-grade glial and glioneuronal tumors that have alterations exclusively within a single molecular pathway [20,30], RGNT seem to be a multiple-pathway disease, a fact that is more characteristic for high-grade tumors. Furthermore, PI3K/AKT/mTOR pathway alterations have been associated with clinical and histologic aggressiveness in LGG [22] as well as poor outcome in patients with RGNT [7]. However, clinical follow-up data of our series appear in line with the current WHO grade I designation.

Our findings also have important implications for treatment management of patients with subtotaly resected or recurrent tumors. Highly potent inhibitors of *FGFR1*, several of which are currently in various phases of clinical development [15], may be valuable treatments for these patients. Similarly, mutations in *PIK3CA* and *NF1* might also be targeted with specific inhibitors of the PI3K and MAPK pathways. However, this will need confirmation in clinical trials.

In conclusion, our findings provide new insight into the molecular genetic background of RGNT and suggest that RGNTs are highly linked to combined MAPK and PI3K/AKT/mTOR signaling pathway activation via concomitant mutations in *FGFR1* and *PIK3CA*, thereby offering options for targeted therapies.

## **Acknowledgements**

We thank V. Zeller, U. Lass and J. Meyer for excellent technical support and the microarray unit of the DKFZ Genomics and Proteomics Core Facility for providing Illumina DNA methylation array-related services. D. Jones is supported by the Everest Centre for Low-grade Paediatric Brain Tumours (The Brain Tumour Charity, UK).

## References

1. Allinson KS, O'Donovan DG, Jena R, Cross JJ, Santarius TS (2015) Rosette-forming glioneuronal tumor with dissemination throughout the ventricular system: a case report. *Clin Neuropathol* 34:64-69. doi:10.5414/NP300682
2. Anan M, Inoue R, Ishii K et al. (2009) A rosette-forming glioneuronal tumor of the spinal cord: the first case of a rosette-forming glioneuronal tumor originating from the spinal cord. *Hum Pathol* 40:898-901. doi:10.1016/j.humpath.2008.11.010
3. Cachia D, Prado MP, Theeler B, Hamilton J, McCutcheon I, Fuller GN (2014) Synchronous rosette-forming glioneuronal tumor and diffuse astrocytoma with molecular characterization: a case report. *Clin Neuropathol* 33:407-411. doi:10.5414/NP300767
4. Capper D, Jones DTW, Sill M et al. (2018) DNA methylation-based classification of central nervous system tumours. *Nature* 555:469-474. doi:10.1038/nature26000
5. Ellezam B, Theeler BJ, Luthra R, Adesina AM, Aldape KD, Gilbert MR (2012) Recurrent PIK3CA mutations in rosette-forming glioneuronal tumor. *Acta Neuropathol* 123:285-287. doi:10.1007/s00401-011-0886-z
6. Gessi M, Lambert SR, Lauriola L, Waha A, Collins VP, Pietsch T (2012) Absence of KIAA1549-BRAF fusion in rosette-forming glioneuronal tumors of the fourth ventricle (RGNT). *J Neurooncol* 110:21-25. doi:10.1007/s11060-012-0940-2
7. Gessi M, Moneim YA, Hammes J et al. (2014) FGFR1 mutations in Rosette-forming glioneuronal tumors of the fourth ventricle. *J Neuropathol Exp Neurol* 73:580-584. doi:10.1097/NEN.0000000000000080
8. Hovestadt V, Remke M, Kool M et al. (2013) Robust molecular subgrouping and copy-number profiling of medulloblastoma from small amounts of archival tumour material using high-density DNA methylation arrays. *Acta Neuropathol* 125:913-916. doi:10.1007/s00401-013-1126-5
9. Jacques TS, Eldridge C, Patel A et al. (2006) Mixed glioneuronal tumour of the fourth ventricle with prominent rosette formation. *Neuropathol Appl Neurobiol* 32:217-220. doi:10.1111/j.1365-2990.2005.00692.x
10. Jones DT, Hutter B, Jager N et al. (2013) Recurrent somatic alterations of FGFR1 and NTRK2 in pilocytic astrocytoma. *Nat Genet* 45:927-932. doi:10.1038/ng.2682
11. Jones DT, Kocialkowski S, Liu L et al. (2008) Tandem duplication producing a novel oncogenic BRAF fusion gene defines the majority of pilocytic astrocytomas. *Cancer Res* 68:8673-8677. doi:10.1158/0008-5472.CAN-08-2097
12. Karafin M, Jallo GI, Ayars M, Eberhart CG, Rodriguez FJ (2011) Rosette forming glioneuronal tumor in association with Noonan syndrome: pathobiological implications. *Clin Neuropathol* 30:297-300
13. Kemp S, Achan A, Ng T, Dexter MA (2012) Rosette-forming glioneuronal tumour of the lateral ventricle in a patient with neurofibromatosis 1. *J Clin Neurosci* 19:1180-1181. doi:10.1016/j.jocn.2011.12.013
14. Komori T, Scheithauer BW, Hirose T (2002) A rosette-forming glioneuronal tumor of the fourth ventricle: infratentorial form of dysembryoplastic neuroepithelial tumor? *Am J Surg Pathol* 26:582-591
15. Lasorella A, Sanson M, Iavarone A (2017) FGFR-TACC gene fusions in human glioma. *Neuro Oncol* 19:475-483. doi:10.1093/neuonc/now240
16. Lin FY, Bergstrom K, Person R et al. (2016) Integrated tumor and germline whole-exome sequencing identifies mutations in MAPK and PI3K pathway genes in an adolescent with rosette-forming glioneuronal tumor of the fourth ventricle. *Cold Spring Harb Mol Case Stud* 2:a001057. doi:10.1101/mcs.a001057
17. Louis DN, Ohgaki H, Wiestler OD, Cavenee WK (2016) WHO Classification of Tumours of the Central Nervous System. Revised 4th edition edn. IARC, Lyon
18. McPherson A, Hormozdiari F, Zayed A et al. (2011) deFuse: an algorithm for gene fusion discovery in tumor RNA-Seq data. *PLoS Comput Biol* 7:e1001138. doi:10.1371/journal.pcbi.1001138

19. Preusser M, Dietrich W, Czech T, Prayer D, Budka H, Hainfellner JA (2003) Rosette-forming glioneuronal tumor of the fourth ventricle. *Acta Neuropathol* 106:506-508. doi:10.1007/s00401-003-0758-2
20. Qaddoumi I, Orisme W, Wen J et al. (2016) Genetic alterations in uncommon low-grade neuroepithelial tumors: BRAF, FGFR1, and MYB mutations occur at high frequency and align with morphology. *Acta Neuropathol* 131:833-845. doi:10.1007/s00401-016-1539-z
21. Rivera B, Gayden T, Carrot-Zhang J et al. (2016) Germline and somatic FGFR1 abnormalities in dysembryoplastic neuroepithelial tumors. *Acta Neuropathol* 131:847-863. doi:10.1007/s00401-016-1549-x
22. Rodriguez EF, Scheithauer BW, Giannini C et al. (2011) PI3K/AKT pathway alterations are associated with clinically aggressive and histologically anaplastic subsets of pilocytic astrocytoma. *Acta Neuropathol* 121:407-420. doi:10.1007/s00401-010-0784-9
23. Rosenblum MK (2007) The 2007 WHO Classification of Nervous System Tumors: newly recognized members of the mixed glioneuronal group. *Brain Pathol* 17:308-313. doi:10.1111/j.1750-3639.2007.00079.x
24. Sahm F, Schrimpf D, Jones DT et al. (2016) Next-generation sequencing in routine brain tumor diagnostics enables an integrated diagnosis and identifies actionable targets. *Acta Neuropathol* 131:903-910. doi:10.1007/s00401-015-1519-8
25. Schlamann A, von Bueren AO, Hagel C et al. (2014) An individual patient data meta-analysis on characteristics and outcome of patients with papillary glioneuronal tumor, rosette glioneuronal tumor with neuropil-like islands and rosette forming glioneuronal tumor of the fourth ventricle. *PLoS One* 9:e101211. doi:10.1371/journal.pone.0101211
26. Sievers P, Stichel D, Schrimpf D et al. (2018) FGFR1:TACC1 fusion is a frequent event in molecularly defined extraventricular neurocytoma. *Acta Neuropathol* 136:293-302. doi:10.1007/s00401-018-1882-3
27. Sturm D, Witt H, Hovestadt V et al. (2012) Hotspot mutations in H3F3A and IDH1 define distinct epigenetic and biological subgroups of glioblastoma. *Cancer Cell* 22:425-437. doi:10.1016/j.ccr.2012.08.024
28. Thommen F, Hewer E, Schafer SC, Vassella E, Kappeler A, Vajtai I (2013) Rosette-forming glioneuronal tumor of the cerebellum in statu nascendi: an incidentally detected diminutive example indicates derivation from the internal granule cell layer. *Clin Neuropathol* 32:370-376. doi:10.5414/NP300612
29. Xu J, Yang Y, Liu Y et al. (2012) Rosette-forming glioneuronal tumor in the pineal gland and the third ventricle: a case with radiological and clinical implications. *Quant Imaging Med Surg* 2:227-231. doi:10.3978/j.issn.2223-4292.2012.09.03
30. Zhang J, Wu G, Miller CP et al. (2013) Whole-genome sequencing identifies genetic alterations in pediatric low-grade gliomas. *Nat Genet* 45:602-612. doi:10.1038/ng.2611

## Figure legends

**Fig. 1** Rosette-forming glioneuronal tumor (RGNT) by DNA Methylation Profiling. Unsupervised hierarchical clustering of DNA methylation profiles of 30 rosette-forming glioneuronal tumors alongside 106 well-characterized CNS neoplasms encompassing other low-grade glial/glioneuronal tumor entities and control tissue. Shown in a two-dimensional representation of pairwise sample correlations using the 20,000 most variant probes by t-distributed stochastic neighbor embedding (t-SNE) dimensionality reduction. Reference methylation classes: IDH-mutant astrocytoma (A IDH), IDH-mutant oligodendroglioma (O IDH), posterior fossa pilocytic astrocytoma (LGG, PA PF), ganglioglioma (LGG, GG), midline pilocytic astrocytoma (LGG, PA MID), supratentorial/hemispheric pilocytic astrocytoma and ganglioglioma (LGG, PA/GG), diffuse leptomeningeal glioneuronal tumor subgroup 1 (DLGNT\_1), diffuse leptomeningeal glioneuronal tumor subgroup 2 (DLGNT\_2), extraventricular neurocytoma (EVN), dysembryoplastic neuroepithelial tumor (LGG, DNT), rosette-forming glioneuronal tumor (LGG, RGNT) and control tissue white matter (CONTROL).

**Fig 2** Clinicopathological characteristics and recurrent genetic alterations in rosette-forming glioneuronal tumors examined by DNA methylation profiling and targeted next-generation sequencing. M, male; F, female; RGNT, rosette-forming glioneuronal tumor; LGG/LGGNT, low-grade glial/glioneuronal tumor; PA, pilocytic astrocytoma

**Fig. 3** Morphological and immunohistochemical features of rosette-forming glioneuronal tumors. Typical histomorphological features of RGNT showing well-differentiated neurocytic cells forming rosettes and perivascular pseudorosettes (a) with immunoreactivity for synaptophysin (b).

**Supplementary Table 1** Summary of clinicopathological characteristics and key genetic alterations identified in the RGNT cohort.

**Supplementary Table 2** Single nucleotide variants (SNVs), small insertions/deletions/substitutions and splice site variants detected in the RGNT cohort.

**Supplementary Fig. 1** Kaplan–Meier curves for overall survival of methylation class RGNT patients in comparison to reference glioma group patients (pilocytic astrocytoma WHO grade I; diffuse astrocytoma, IDH-mutant, WHO grade II).

**Supplementary Fig. 2** Unsupervised hierarchical clustering of DNA methylation profiles of 30 rosette-forming glioneuronal tumors alongside 106 well-characterized CNS neoplasms encompassing other low-grade glial/glioneuronal tumor entities and control tissue.

**Supplementary Table 1 - Summary of clinicopathological characteristics and key genetic alterations identified in the RGNT cohort**

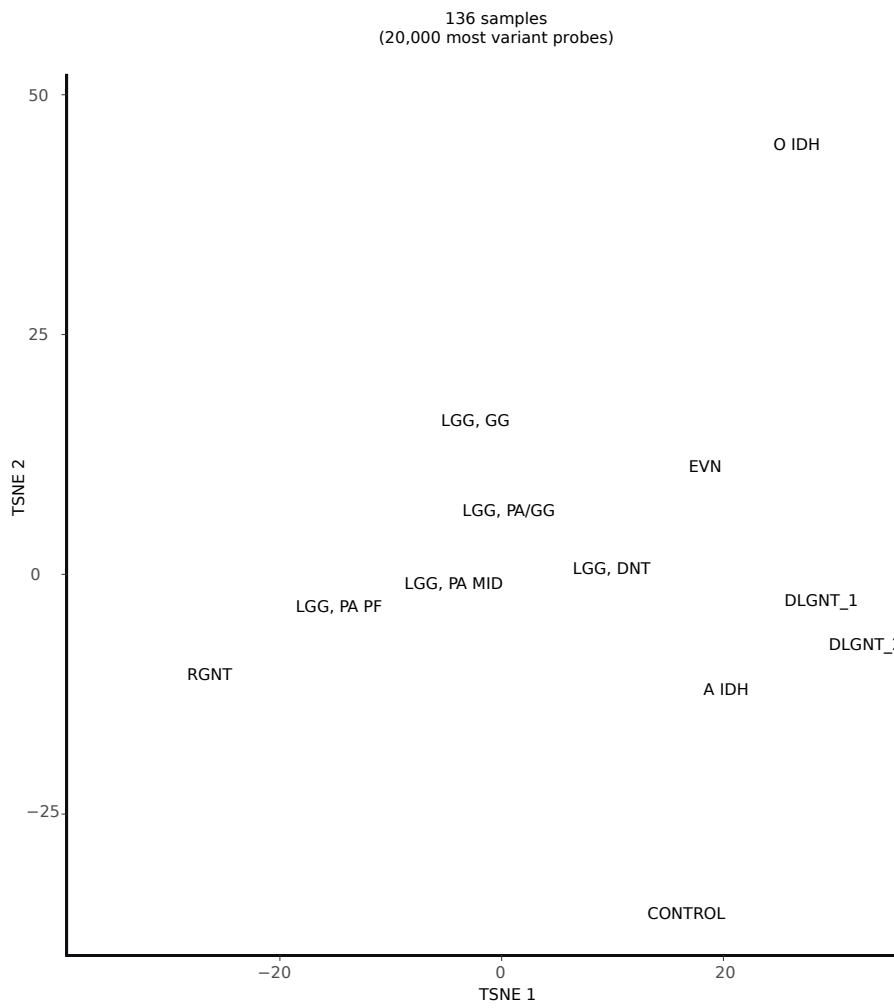
Case #	Age (years)	Sex	Tumor location	Diagnosis	<i>FGFR1</i>	<i>PIK3CA</i>	<i>NF1</i>	<i>PTPN11</i>	Copy number variations
1	12	m	4th ventricle	LGNT	p.N546K	p.H1047R		p.N58H	balanced
2	23	m	4th ventricle	RGNT	p.N546K	p.H1047R	splicing		balanced
3	25	f	Cerebellum	PA	p.N546K	p.H1047R	p.M1149V		balanced
4	43	m	Pineal region	RGNT	p.K656E				gain of chr 7, 12
5	39	m	4th ventricle	LGG	p.K656E				loss of chr 4, 19, 21q
6	28	f	Tectum	PA	p.N546K				balanced
7	69	f	3th ventricle	LGG/LGGNT	p.K656E		p.R1276X and p.N1259S		balanced
8	67	f	Cerebellum	PA	p.N546K				balanced
9	20	f	Cerebellum	LGG	p.N546K	p.H1047R	p.E1790X		balanced
10	31	m	4th ventricle	RGNT	p.N546K	p.H1047R			balanced
11	34	m	4th ventricle	RGNT	p.N546K	p.G1049R			loss of chr 8p, 20p
12	36	f	Thalamus, brainstem	RGNT	p.N546K	p.H1047R	p.W1831X		balanced
13	44	m	3th ventricle	RGNT	p.K656E				balanced
14	55	f	4th ventricle	RGNT	p.N546K				balanced
15	43	m	Cerebellum	PA	p.N546K				gain of chr 5, 6, 7, 8, 11, 12, 20
16	14	f	4th ventricle	RGNT	p.N546K	p.H1047R		p.P491H	balanced
17	24	f	Pineal region	PA	p.N546K	p.H1047R	p.R2637X		balanced
18	21	m	4th ventricle	RGNT	p.N546K	p.E545K			balanced
19	59	m	Cerebellum	PA	p.N546K		p.R897W and p.H647R		gain of chr 6p, segmmetal gain of 2q, 7q, 12q
20	40	m	4th ventricle	RGNT	p.N546K				balanced
21	50	m	Cerebellum	RGNT	p.K656E	p.E542K			balanced
22	10	f	Cerebellum	PA	p.K656E	p.H1047R			balanced
23	20	m	4th ventricle	RGNT	p.K656E	p.H1047R	splicing		balanced
24	38	f	4th ventricle	RGNT	p.N546K	p.H1047R			balanced
25	21	f	Cerebellum	PA	p.N546K	p.H1047R			balanced
26	18	f	4th ventricle	RGNT	p.N546K	p.H1047R	p.R416X		balanced
27	28	f	4th ventricle	RGNT	p.N546K	p.H1047R			balanced
28	41	f	4th ventricle	RGNT	p.K656E		p.E1264G and p. L1161V		balanced
29	25	m	Cerebellum	RGNT	p.N546K	p.H1047L			balanced
30	21	m	Cerebellum	RGNT	p.N546K	p.E545K			balanced

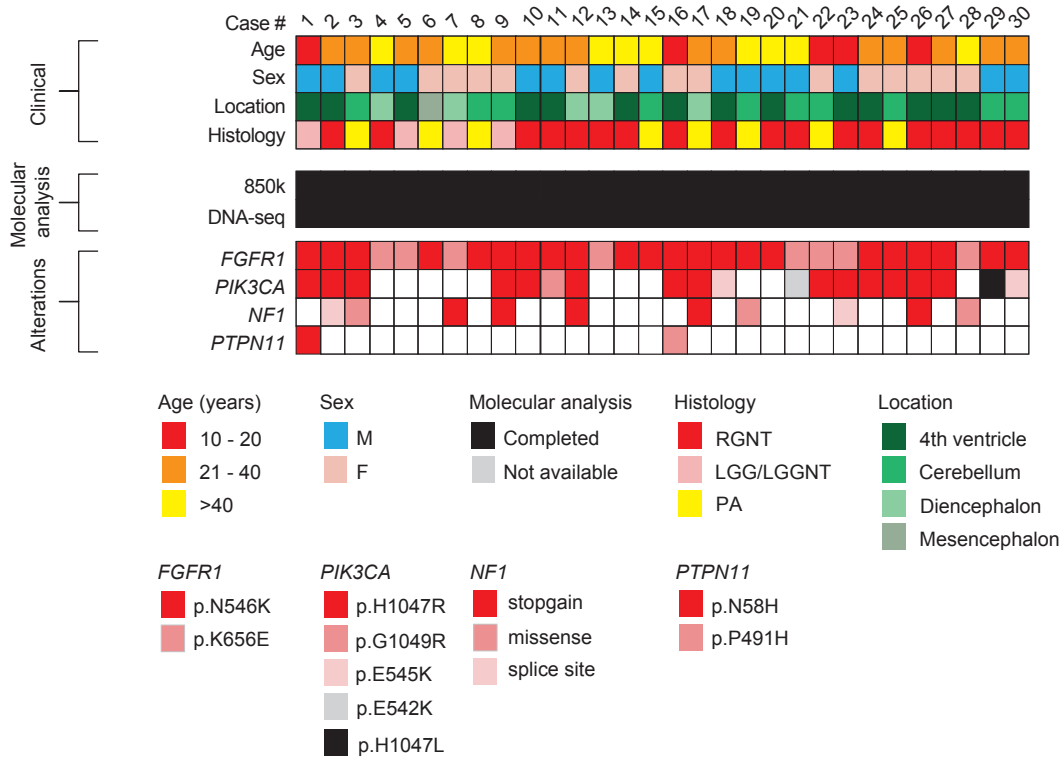
Abbreviations: m, male; f, female; RGNT I, rosette-forming glioneuronal tumor WHO grade I; PA I, pilocytic astrocytoma WHO grade I; LGG, low-grade glioma; LGGNT, low-grade glioneuronal tumor; chr, chromosome

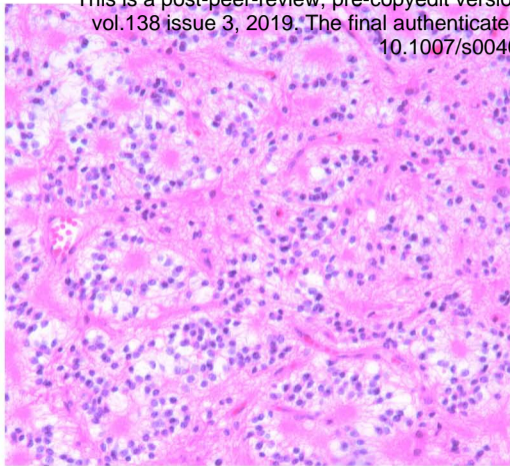
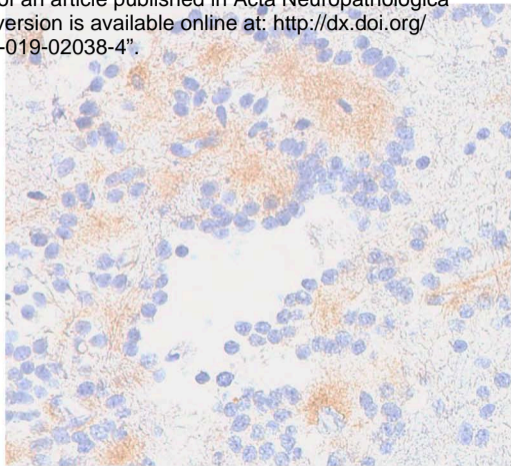










**a****b**

“This is a post-peer-review, pre-copyedit version of an article published in *Acta Neuropathologica* vol.138 issue 3, 2019. The final authenticated version is available online at: <http://dx.doi.org/10.1007/s00401-019-02038-4>”.

